Ballistic annihilation kinetics: The case of discrete velocity distributions

P. L. Krapivsky and S. Redner
Center for Polymer Studies and Department of Physics, Boston University, Boston, Massachusetts 02215

F. Leyvraz
Instituto de Física–Universidad Nacional Autónoma de Mexico, Laboratorio de Cuernavaca, Apartado Postal 20-364, 01000 México, Distrito Federalé, Mexico

(Received 16 December 1994)

The kinetics of the annihilation process $A+A\rightarrow\emptyset$ with ballistic particle motion is investigated when the distribution of particle velocities is *discrete*. This discreteness is the source of many intriguing phenomena. In the mean field limit, the densities of different velocity species decay in time with different power law rates for many initial conditions. For a one-dimensional symmetric system containing particles with velocity 0 and ± 1, there is a particular initial state for which the concentrations of all three species decay as $t^{-2/3}$, where t is the time. For the case of a fast "impurity" in a symmetric background of $+$ and $-$ particles, the impurity survival probability decays as $\exp(-\text{const}\times\ln^2 t)$. In a symmetric four-velocity system in which there are particles with velocities $\pm v_1$ and $\pm v_2$, there again is a special initial condition where the two species decay at the same rate $t^{-\alpha}$, with $\alpha\cong 0.72$. Efficient algorithms are introduced to perform the large-scale simulations necessary to observe these unusual phenomena clearly.

PACS number(s): 02.50.−r, 82.20.Pm, 03.20.+i, 05.20.Dd

I. INTRODUCTION

In this article, we describe some intriguing aspects of the reaction kinetics in single species annihilation $A+A\rightarrow\emptyset$ when particles move ballistically with a *discrete* distribution of velocities. Unexpected long-time phenomena occur that depend fundamentally on the form of the initial velocity distribution. The results discussed here are complementary to our earlier work on ballistic annihilation with a continuous distribution of particle velocities [1]. For this latter system, the exponents characterizing the decay of the concentration and the typical velocity depend continuously on the form of the initial velocity distribution. For discrete velocity distributions, however, the decay kinetics exhibits a fundamentally richer character with fundamental differences in long-time behavior for small changes in the initial conditions.

Our investigation is also inspired by earlier work by Elskens and Frisch and independently Krug and Spohn, who considered the kinetics of the "two-velocity," or "±," model in one dimension [2]. Here the initial velocity distribution of reactants is

$$P(v,t=0)=p_+\delta(v-v_0)+p_-\delta(v+v_0)\ ,$$

with $p_+ + p_- = 1$. The spatial distribution of reactants has minimal influence on the kinetics as long as the distribution is nonsingular. For convenience, we therefore consider the distribution to be Poisson in this paper. When $p_+ > p_-$, the majority species quickly reaches a finite asymptotic limit, while the minority density decays exponentially in time. In the interesting situation where the initial densities of the two species are equal, the density decays as [2]

$$c(t)\propto\sqrt{c(0)/v_0 t} \qquad (1)$$

in the long-time limit. This relatively slow decay, compared to the rate equation prediction of t^{-1}, stems from initial density fluctuations. In a region of length L there will typically be an imbalance of the order of $\sqrt{L}$ in the number of $+$ and $-$ particles. After a time $t\cong L$ has elapsed, only this initial number difference will remain within the region. Therefore the local particle number is proportional to $\sqrt{L}$ and Eq. (1) follows. Thus the system organizes into domains of like velocity particles whose typical size grows linearly in time as the reaction proceeds (Fig. 1).

Consider now a simple and natural generalization to the three-velocity model [3]. Without loss of generality, the initial distribution of velocities may be written as

$$P(v,t=0)=p_+\delta(v-v_+)+p_-\delta(v+1)+p_0\delta(v)\ , \qquad (2)$$

with $p_+ + p_- + p_0 = 1$. We will primarily focus on the symmetric case where $v_+ = 1$ and $p_+ = p_- = p_\pm$. The space-time evolution of this system in one dimension for two representative values of $(p_\pm, p_0)$ is shown in Fig. 1. One of our basic goals is to understand the time dependence of the mobile and stationary concentrations for different initial conditions. Particularly intriguing is the transition from a regime where the stationary particles persist, for $p_0 > \frac{1}{4}$, to a regime where stationary particles decay more rapidly than the mobile particles, for $p_0 < \frac{1}{4}$. At a "tricritical" point located at $p_0 = \frac{1}{4}$, the concentrations of both the mobile and stationary species decay as $t^{-2/3}$ [4]. While there is now a theoretical approach to compute this exponent exactly [5], there is not yet an intuitive understanding of this striking behavior. Another intriguing facet of this system is the decay of a "fast impurity," namely, a single particle with velocity $+1$ in a system with equal concentrations of 0 and -1 particles.

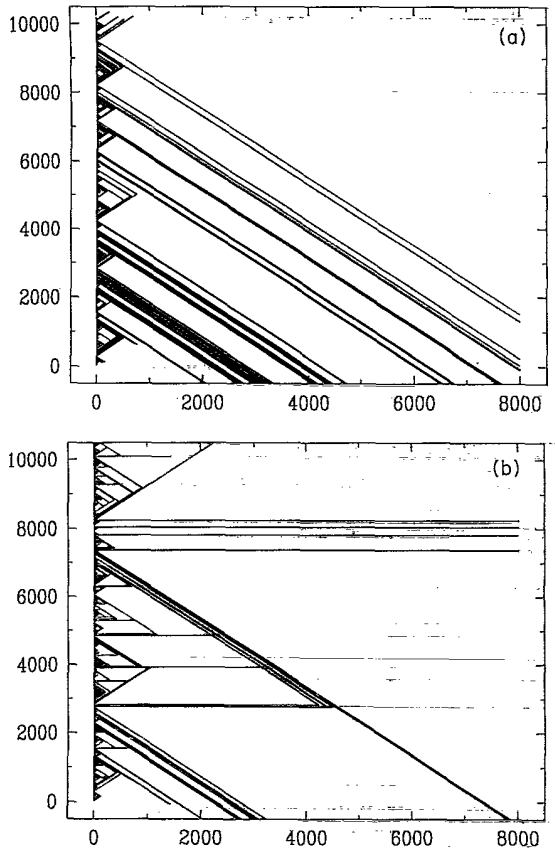

FIG. 1. Space-time representation of particle trajectories in the symmetric two- and three-velocity models, where particles move with velocity 0 or ± 1. Shown are (a) $p_0=0.0$, $p_\pm=0.50$ and (b) $p_0=0.25$, $p_\pm=0.375$.

By considering the dominant contributions to the impurity survival probability, we find that this quantity decays asymptotically as $\exp(-\text{const}\times\ln^2 t)$.

Another class of interesting behavior is exemplified by the symmetric four-velocity model with initial velocity distribution

$$P(v,t=0)=p_1(\delta(v-v_1)+\delta(v+v_1)) +p_2(\delta(v-v_2)+\delta(v+v_2)) , \quad (3)$$

with $v_2>v_1$ and $p_1+p_2=1$. According to the rate equations, the more mobile species decays as t^{-v_2/v_1} while the less mobile one decays as t^{-1}, independent of the initial concentrations. In one dimension, however, either the slower or the faster particles dominate in the long-time limit, depending on their relative initial concentrations. At a critical value of p_1/p_2, which depends on v_1/v_2, numerical simulations indicate that both species decay as $t^{-\alpha}$, with $\alpha\cong 0.72$. We shall also argue that systems with symmetric velocity distributions with $n>4$ components exhibit behavior that is characteristic of either the three-velocity model, if n is odd, or the four-velocity model, if n is even. Thus we focus primarily on three- and four-velocity models as the simplest in the family of symmetric discrete velocity models.

In Secs. II and III we discuss the annihilation kinetics of discrete velocity models in the mean field limit. We first treat the conventional rate equations, which are based on one-dimensional kinematics. The shortcoming inherent in the assumption naturally leads us to consider "constant speed" models and the correct d-dimensional kinematics. We find a rich kinetic behavior that depends on the ratios of initial concentrations, the particle radii, and the speeds of the different species. In Sec. IV we study the kinetics of one-dimensional systems. Given the subtle nature of many of our observations, relatively efficient and specialized algorithms were developed to provide sufficient data to determine the long-time behavior with confidence. For the symmetric three-velocity model, we investigate in detail the $t^{-2/3}$ decay associated with the tricritical point and the $\exp(-\text{const}\times\ln^2 t)$ decay of the fast impurity problem. We then consider the kinetics of the symmetric four-velocity model, once again concentrating on the multicritical behavior associated with the initial condition where both the fast and the slow particles decay at the same rate.

II. MEAN FIELD THEORY WITH ONE-DIMENSIONAL KINEMATICS

A. The three-velocity model

The mean-field rate equations for the three-velocity model are deceptively simple, but lead to relatively complex behavior. For symmetric velocity distribution, the rate equations for the concentrations of the left-moving, right-moving, and stationary species, $c_-(t)$, $c_+(t)$, and $c_0(t)$, respectively, are

$$\begin{aligned}\dot c_0&=-c_0(c_++c_-)\,,\\ \dot c_+&=-c_+(c_0+2c_-)\,,\\ \dot c_-&=-c_-(c_0+2c_+)\,,\end{aligned} \quad (4)$$

where the overdot denotes time derivative. The numerical factors of 2 reflect the fact that the rate of a $+-$ collision is twice that of $+0$ or -0 collisions, if we assume that particles move only in one dimension. It is in this spirit that the above rate equations are referred to as mean field theory with one-dimensional kinetics. A more complete approach that incorporates d-dimensional kinematics will be outlined in Sec. III.

To solve these equations, it is helpful to rewrite the rate equations in terms of $\psi\equiv(c_++c_-)/c_0$ and $\phi\equiv(c_+-c_-)/c_0$ and the modified time $dx\equiv c_0 dt$. This gives

$$\psi'+\psi=\phi^2,\quad \phi'+\phi=\phi\psi\,, \quad (5)$$

where the prime denotes differentiation with respect to x. Use of the integrating factors $\Psi=\psi e^x$ and $\Phi=\phi e^x$ simplify these equations to

$$\Psi'=\Phi^2 e^{-x},\quad \Phi'=\Phi\Psi e^{-x}\,, \quad (6)$$

from which it is evident that $\Psi^2-\Phi^2=\text{const}\equiv a^2>0$. Thus the equation of motion for Ψ becomes $\Psi'=e^{-x}(\Psi^2-a^2)$, with the solution

$$\Psi(y)=a\coth\left[\coth^{-1}\left[\frac{\Psi(0)}{a}\right]-ay\right], \tag{7}$$

where we have introduced the timelike variable $dy=e^{-x}dx$, with $y=1-e^{-x}$ a monotone increasing function of t.

To classify the long-time behavior, consider the relative composition triangle $p_+ + p_- + p_0 = 1$. As indicated in Fig. 2, a given initial condition typically evolves to a "phase" where only a single species persists in the long-time limit. Consider first the stationary, or "0," phase $c_0(\infty)>0$. From the definitions of x and y, the condition $c_0(\infty)>0$ implies that $y\sim 1-e^{-at}$ as $t\to\infty$, which leads to $\psi\sim e^{-at}$. Thus the concentrations of the mobile species decay exponentially in time in the 0 phase. Interestingly, for $p_+ = p_-$ stationary particles persist even if the initial concentration of stationary particles becomes small. However, the width of this phase becomes vanishingly small in this limit. To determine this width, note, from Eq. (4), that on the boundary where the densities of the stationary and positive particles decay at the same rate, the asymptotic solutions of the rate equations are $c_+, c_0 \propto 1/t$, while $c_-\sim 1/t^3$. Thus the boundary between the 0 and + phases can be identified by the ratio ψ approaching a finite limit as $t\to\infty$. Since $1-y$ approaches 0 as $t\to\infty$, a finite limiting value for $\psi = e^{-x}\Psi$ requires that the argument of the hyperbolic cotangent in Eq. (7) goes to zero. One thereby finds that the width of the 0 phase region vanishes as $\exp[-1/c_0(0)]$ as $c_0(0)\to 0$.

For the symmetric system, a detailed computation gives the asymptotics

$$\begin{aligned} c_\pm &\sim \tfrac{1}{2}c_0(\infty)G(\lambda)e^{-c_0(\infty)t}, \\ c_0(t) &\sim c_0(\infty)\exp[G(\lambda)e^{-c_0(\infty)t}], \end{aligned} \tag{8}$$

with $G(\lambda)\equiv\exp[\int_1^\lambda (dz/z)e^{-z} - \int_0^1 (dz/z)(1-e^{-z})]$, $\lambda\equiv 2c_\pm(0)/c_0(0)$, and the final density of stationary particles given by

$$c_0(\infty)=c_0(0)e^{-2c_\pm(0)/c_0(0)}. \tag{9}$$

Thus, while a residue of stationary particles always persists, their concentration is astronomically small if the initial concentration of stationaries is small.

For the asymmetric three-velocity model, the corresponding rate equations are

$$\begin{aligned} \dot c_0 &= -c_0(vc_+ + c_-), \\ \dot c_+ &= -c_+[vc_0 + (1+v)c_-], \\ \dot c_- &= -c_-[c_0 + (1+v)c_+]. \end{aligned} \tag{10}$$

While we are unable to solve these equations, we can readily find the asymptotic behavior. In the 0 phase, the rate equations for the mobile particles have the asymptotic solutions $c_+(t)\sim e^{-tvc_0(\infty)}$ and $c_-(t)\sim e^{-tc_0(\infty)}$. Similar exponential decays characterize the behavior of the minority species in the other two phases. On the separatrices, however, two species decay at the same rate while the minority species decays faster. For example, on the separatrix between the 0 and + phases, one has $c_0\sim c_+ \gg c_-$. Substituting this into Eq. (10) yields the asymptotic solution $c_+, c_0 \simeq 1/vt$, while $c_-\sim t^{-1-2/v}$. Similarly, on the separatrix between the 0 and − phases $c_-, c_0 \simeq 1/t$ and $c_+\sim t^{-1-2v}$.

The long-time persistence of stationary particles also occurs in a general $(2m+1)$-component model with velocities $0=v_0<v_1<\cdots<v_m$ and corresponding concentrations $c_0(t), c_1(t), \ldots, c_m(t)$. The rate equations for these concentrations are

$$\begin{aligned} \dot c_0 &= -2c_0\sum_{j=1}^{m} v_j c_j, \\ \dot c_k &= -c_0 c_k v_k - 2c_k\left[v_k\sum_{j=1}^{k-1} c_j + \sum_{j=k}^{m} v_j c_j\right]. \end{aligned} \tag{11}$$

Introducing $x=\int_0^t dt' c_1(t')$ and the dimensionless concentrations $\phi_k = c_k/c_0$, we obtain a closed system of equations for $\phi_k(x)$ and an additional equation for $c_0(x)$

$$\begin{aligned} \frac{d\ln\phi_k}{dx} &= -v_k - 2\sum_{j=1}^{k-1}(v_k - v_j)\phi_j, \quad k=1,\ldots,m, \\ \frac{d\ln c_0}{dx} &= -2\sum_{j=1}^{m} v_j\phi_j. \end{aligned} \tag{12}$$

Since $v_k > v_j$ for $k>j$, the first of Eqs. (12) gives $\phi_k(x)\le\phi_k(0)e^{-v_k x}$. Substituting these into the equation for c_0 yields

$$\ln\frac{c_0(x)}{c_0(0)} \ge -2\sum_{j=1}^{m}\phi_j(0)(1-e^{-v_j x}), \tag{13}$$

which immediately leads to the lower bound for final density of stationary particles

$$c_0(\infty)\ge c_0(0)\exp\left[-\frac{2}{c_0(0)}\sum_{j=1}^{m} c_j(0)\right]. \tag{14}$$

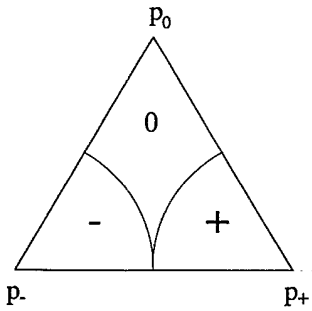

FIG. 2. Phase diagram of the symmetric three-velocity model in the mean field limit within the relative compositon triangle defined by triangular region $p_+ + p_- + p_0 = 1$. The regions marked by +, −, and 0 are phases where only positive, negative, or stationary particles, respectively, persist in the long-time limit. Along the boundaries between +0 or −0, the concentrations of the two competing species decay as t^{-1}, while the minority species decays as t^{-3}. The width of the 0 phase region is vanishingly small as $p_0\to 0$.

For the three-velocity case this bound is exact and coincides with Eq. (9). Thus stationary particles always survive in the symmetric $(2m+1)$-velocity model, although the final residue is vanishingly small when their initial concentration is small.

B. The four-velocity model

For the symmetric four-velocity model, denote by c_1 and c_2 the concentrations of species with velocities $\pm v_1$ and $\pm v_2$, respectively. Without loss of generality, let $v_2 > v_1$ and set $v_1 = 1$, $v_2 = v$. The rate equations for this system are

$$\dot{c}_1 = -2c_1^2 - 2vc_1c_2, \quad \dot{c}_2 = -2vc_2^2 - 2vc_1c_2 , \tag{15}$$

with the asymptotic solution

$$c_1(t) \sim t^{-1}, \quad c_2(t) \sim t^{-v} . \tag{16}$$

Thus the faster species decays nonuniversally as t^{-v}. This asymptotic behavior is reached only at very long times, however, when the initial velocities are nearly identical. Essentially the same equations were solved in the context of heterogeneous diffusive single-species annihilation in which particles have different diffusion coefficients [6].

Analogous behavior occurs in the symmetric $2m$-velocity model with concentrations $c_1(t), \ldots, c_m(t)$ and speeds $\pm v_j$, with $v_1 < \cdots < v_m$. The rate equations are

$$\dot{c}_k = -2c_k \left[v_k \sum_{j=1}^{k-1} c_j + \sum_{j=k}^{m} v_j c_j \right] . \tag{17}$$

Introducing now $x = 2\int_0^t dt' c_1(t')$ and $\phi_k = c_k/c_1$, $\phi_1 \equiv 1$, we obtain

$$\begin{aligned} \frac{d\ln\phi_k}{dx} &= -\sum_{j=1}^{k-1} (v_k - v_j)\phi_j, \quad 2 \le k \le m , \\ \frac{d\ln c_1}{dx} &= -\sum_{j=1}^{m} v_j \phi_j . \end{aligned} \tag{18}$$

As in the $(2m+1)$-velocity model, one can straightforwardly derive $\phi_k(x) \le \phi_k(0) e^{-(v_k - v_1)x}$. This, together with the equation for c_1 and the relation $\phi_1 \equiv 1$, shows that $c_1 \sim e^{-v_1 x}$. Combining this result with the definition of x proves that $x \to \infty$ as $t \to \infty$. It therefore follows that in the long-time limit $\phi_k(x) \sim e^{-(v_k - v_1)x}$. Reexpressing this in terms of $c_j(t)$ leads to

$$c_1 \sim t^{-1}, \; c_2 \sim t^{-v_2/v_1}, \ldots, c_m \sim t^{-v_m/v_1} . \tag{19}$$

Thus a more mobile species k decays nonuniversally with an associated exponent equal to the velocity ratio v_k/v_1.

III. MEAN FIELD THEORY WITH d-DIMENSIONAL KINEMATICS

We now generalize the rate equations to account for d-dimensional kinematics. This should be viewed as the "true" mean field theory of ballistic annihilation. It is convenient to consider first the kinetics of a single impurity in a background of particles moving at the same speed. From this, the general mean field theory follows naturally.

A. The impurity limit

Let background particles of radii R move with identical velocities $\mathbf{v}$, which are uniformly distributed in angle, i.e., $P(\mathbf{v}, t=0) = \delta(|\mathbf{v}| - v_0)$. If we temporarily neglect the annihilation events among background particles, then by an elementary mean free path argument, the (infinitesimal) concentration of the impurity species with radius R_I varies as

$$\dot{c}_I = -c_I c v \Omega_{d-1}(R + R_I) , \tag{20}$$

where $\Omega_{d-1}(R)$ is the volume of a sphere of radius R in $d-1$ dimensions.

If the impurity moves with velocity $\mathbf{w}$, then the decay rate must be averaged overall directions of relative velocities $\mathbf{v} - \mathbf{w}$. This leads to

$$\begin{aligned} \dot{c}_I &= -c_I c v \Omega_{d-1}(R + R_I) \\ &\quad \times \frac{\int_0^\pi d\theta (\sin\theta)^{d-1} \sqrt{1 + \epsilon^2 + 2\epsilon\cos\theta}}{\int_0^\pi d\theta (\sin\theta)^{d-2}} \\ &\equiv -c_I c v \Omega_{d-1}(R + R_I)\mathcal{F}(\epsilon) \end{aligned} \tag{21}$$

with $\epsilon = w/v$. To find the impurity concentration c_I we must first determine the background concentration c. Since a background particle can be considered as an impurity of radius R moving with velocity v, we apply Eq. (21) to obtain $\dot{c} = -c^2 v \Omega_{d-1}(2R)\mathcal{F}(1)$, with the asymptotic solution $c(t) \sim [v\Omega_{d-1}(2R)\mathcal{F}(1)t]^{-1}$. Using this in Eq. (21) gives

$$c_I \sim t^{-\alpha} \text{ with } \alpha = \alpha(R_I, \epsilon) = \frac{\Omega_{d-1}(R + R_I)\mathcal{F}(\epsilon)}{\Omega_{d-1}(2R)\mathcal{F}(1)} . \tag{22}$$

For example, when there is a stationary particle in a uniform background of moving particles, $c_I \sim t^{-\alpha_0(d)}$, with

$$\alpha_0(d) = \mathcal{F}(0)/\mathcal{F}(1) = \frac{\Gamma(\frac{1}{2})\Gamma(d - \frac{1}{2})}{2^{d-1}\Gamma^2(d/2)} , \tag{23}$$

and Γ is the gamma function. Note that $\alpha_0(d)$ is rational for odd dimensions and transcendental for even dimensions: $\alpha_0(1) = 1$, $\alpha_0(2) = \pi/4$, $\alpha_0(3) = \frac{3}{4}$, etc. Interestingly, $\alpha_0(\infty) = 1/\sqrt{2}$, which can be understood by noting that in the limit $d \to \infty$, two arbitrary particles always move orthogonally with relative velocity $v\sqrt{2}$. The expression for $\alpha_0(\infty)$ [Eq. (22)] essentially involves the inverse of this factor.

B. Stationary and moving species

Consider now the d-dimensional analog of the symmetric three-velocity model in which there is a finite initial concentration of stationary particles of radii R_0 and mobile particles of radii R all moving with speeds v. The appropriate rate equations for the corresponding concen-

trations $c_0(t)$ and $c(t)$ are similar to those for the above impurity limit except that one must account for the influence of stationary particles on moving particles. The rate equations become [compare with Eqs. (4) with $c_+ = c_-$]

$$\dot{c} = -v\Omega_{d-1}(R+R_0)c_0 c \ , \qquad \dot{c} = -v\Omega_{d-1}(R+R_0)[c_0 c + \lambda_d c^2] \ , \tag{24}$$

where $\lambda_d = \mathcal{I}(1)\Omega_{d-1}(2R)/\Omega_{d-1}(R+R_0)$. Introducing the modified time variable $T = v\Omega_{d-1}(R+R_0) \times \int_0^t dt' c(t')$ gives the linear equations

$$\frac{dc_0}{dT} = -c_0, \quad \frac{dc}{dT} = -c_0 - \lambda_d c \ , \tag{25}$$

which can be readily solved to give

$$c_0(T) = c_0(0)e^{-T} \ , \qquad c(T) = c(0)e^{-\lambda_d T} - c_0(0)\frac{e^{-T} - e^{-\lambda_d T}}{\lambda_d - 1} \ . \tag{26}$$

For $\lambda_d \geq 1$, the concentration of the mobile species decays exponentially in real time t while stationary particles always persist:

$$c_0(\infty) = c_0(0)\left[1 + (\lambda_d - 1)\frac{c(0)}{c_0(0)}\right]^{-1/(\lambda_d - 1)} \ . \tag{27}$$

For $\lambda_d < 1$, there are three different regimes. For small initial concentration of mobile species $c(0) < 1/(2-\lambda_d)$, the density of moving particles decays exponentially in time, while stationary particles persist with a residue still given by Eq. (27). At the critical point $c(0) = 1/(2-\lambda_d)$ and $c_0(0) = (1-\lambda_d)/(2-\lambda_d)$, both species decay as t^{-1}. Finally, for $c(0) > 1/(2-\lambda_d)$, both species decay as distinct power laws in time: $c(t) \sim t^{-1} \gg c_0(t) \sim t^{-1/\lambda_d}$. (Amusingly, these same three qualitative regimes occur in the one-dimensional three-velocity system.) For example, in three dimensions, $\lambda_3 = \sqrt{24}[2R/(R+R_0)]^2$; hence the threshold between different behaviors $\lambda_3 = 1$ occurs when $R_0/R \cong 3.42673$. Thus the stationary particles always persist if their relative size is small $R_0/R \leq 3.42673$, while for $R_0/R > 3.42673$ stationary particles may disappear if their initial concentration is small enough.

C. The two-speed model

For the d-dimensional two-speed model, with c_j, R_j, and v_j the concentration, radius, and speed of the jth species, $j = 1,2$, with $\epsilon \equiv v_1/v_2 < 1$, the rate equations are

$$\dot{c}_1 = -c_1^2 - \mu c_1 c_2, \quad \dot{c}_2 = -\mu c_1 c_2 - \nu c_2^2 \ , \tag{28}$$

where we have set $v_1\Omega_{d-1}(2R_1)\mathcal{I}(1) = 1$ by rescaling the time and have introduced

$$\mu = \epsilon^{-1}\frac{\Omega_{d-1}(R_1+R_2)}{\Omega_{d-1}(2R_1)}\frac{\mathcal{I}(\epsilon)}{\mathcal{I}(1)}, \quad \nu = \epsilon^{-1}\frac{\Omega_{d-1}(R_2)}{\Omega_{d-1}(R_1)} \ . \tag{29}$$

Equations (28) give rise to three asymptotic behaviors that depend on the relative magnitudes of μ and ν:

$$\begin{aligned} &c_1(t) \sim t^{-1}, \ c_2(t) \sim t^{-\mu} \ , \ 1 < \nu < \mu \ , \\ &c_1(t) \sim t^{-\mu/\nu}, \ c_2(t) \sim t^{-1}, \ \nu < \mu < 1 \ , \\ &c_1(t) \sim t^{-1}, \ c_2(t) \sim t^{-1}, \ \nu < \mu < 1, \ \mu < 1 < \nu \ . \end{aligned} \tag{30}$$

In the two remaining cases of $1 < \nu < \mu$ and $\nu < 1 < \mu$ the asymptotic behavior depends also on initial concentrations. The first and the second asymptotics are realized when $(\mu-1)/(\mu-\nu) \gtrless c_2(0)/c_1(0)$, respectively, while the third asymptotics occurs if $(\mu-1)/(\mu-\nu) = c_2(0)/c_1(0)$. Parenthetically, for an arbitrary number of mobile species of equal radii in three dimensions, a similar analysis gives

$$c_j(t) \sim t^{-\mu_j}, \quad \mu_j = \frac{v_1}{4v_j} + \frac{3v_j}{4v_1} \ , \tag{31}$$

where v_1 is the smallest velocity (therefore, $\mu_1 \equiv 1$). Thus the least mobile species decays as t^{-1}, while the more mobile species decay nonuniversally.

IV. KINETICS IN ONE DIMENSION

A. Geometric approach for the symmetric two-velocity model

For completeness and to provide a framework to discuss the three- and four-velocity models, we first give a geometric derivation for the decay of the concentration in the two-velocity or $\pm$ model when the initial concentrations of the two species are equal. This approach is based on the equivalence between the kinetics of the particle system and the smoothing of one-dimensional stepped interface (Fig. 3). In this mapping, a right-moving particle in the $\pm$ model is equivalent to an "up" step in the corresponding interface. This up step moves to the right at the same speed as the initial particle. Similarly, a left-moving particle is equivalent to a left-moving "down" interface step. An annihilation event in the par-

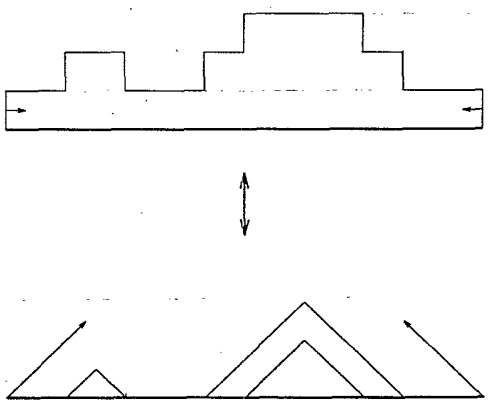

FIG. 3. Equivalence between the time evolution of the two-velocity model and a one-dimensional "wedding cake" interface. The collision partner of the initial particle is indicated in both the particle and the interface representations by the small arrows.

ticle system corresponds to the disappearance of a tier in the interface. Clearly, the collision partner of a given up step is the first down step to the right, which is at the same height as the initial step.

Since up and down steps are uncorrelated and occur with equal probability, the probability f_n that the initial up step (defined to be particle 0) collides with its $(2n+1)$st neighbor is exactly equal to the first passage probability for a random walk to return to the origin at $2n+2$ steps. Thus the initial right-moving particle annihilates with a left-moving $(2n+1)$st particle with probability [7]

$$f_n = 2^{-2n-1}\frac{(2n)!}{n!(n+1)!} \qquad (32)$$

Asymptotically, this collision probability varies as $n^{-3/2}$ as $n\to\infty$. Consequently, the probability that the initial particle survives potential encounters up to the $2n$th neighbor $S_n \equiv 1-\sum_{n'\le n} f_{n'}$ leads to a survival probability that decays as $S_n \sim n^{-1/2}$, or $c(t)\sim t^{-1/2}$ in the continuum limit.

B. The three-velocity model

For the three-velocity model, there does not appear to be a similar geometric construction to help determine the kinetics. We therefore resort to qualitative arguments, as well as numerical simulations, to determine the long-time behavior. In one dimension, we expect the kinetics to be different from mean field predictions because of the tendency of like velocity particles to cluster, as observed in space-time graphs (Fig. 1). For concreteness, we focus on the symmetric system where $p_+ = p_- \equiv p_\pm$ and first investigate whether stationary particles persist for any value of p_0 by numerical simulations. Because of subtle crossover effects, a direct molecular dynamics approach is inadequate to yield accurate results and we therefore developed a more efficient approach in which all collision partners and corresponding collision times are identified at the outset.

In this algorithm, stationary or right-moving particles are placed on a stack (first in, last out) as they are initially created. When a left-moving particle is created, its collision partner is determined immediately, since this partner is necessarily one of the particles from the already existing stack. (There is a particular case in which a negative velocity particle is deposited when the stack is empty. This exits the system, since free boundary conditions are employed. To ensure that this effect does not give spurious results, only particles from the middle half of the system are considered.) The determination of the collision partner of the left-moving particle is accomplished by straightforward comparisons. If the uppermost particle on the stack moves to the right, then it is the collision partner and the collision time is recorded. On the other hand, if the "last" particle on the stack has zero velocity, one must compare the collision time between this last particle on the stack and the left-moving particle, and the collision time between the last particle with "earlier" outgoing particles from the stack. All collision partners and corresponding collision times are determined up to and including the collision time of the initial left-moving particle. Right-moving or stationary particles for which the collision time is determined are then removed from the stack. From the stored array of collision times one determines $c_\pm(t)$ and $c_0(t)$ by counting the number of particles of a given species that survive at that time.

With this method we simulated 5×10^5 particles to 10^5 time steps in approximately 30 CPU s on a DEC/AXP 3000/400 computer workstation. Our numerical results are typically based on 100 realizations at each initial concentration. These simulations reveal the following basic results (Fig. 4): For $p_0 < \frac{1}{4}$, $c_0(t)\sim 1/t$ and $c_\pm(t)\sim t^{-1/2}$. The crossover to the asymptotic behavior becomes progressively more gradual as $p_0\to\frac{1}{4}$ from below and there is a substantial time range for which $c_\pm(t)$ and $c_0(t)$ decay at nearly the same rate before the final asymptotics is reached. (This is the primary reason for the erroneously reported nonuniversal behavior based on data from direct and much less extensive molecular dynamics simulations [1].) Exactly at $p_0=\frac{1}{4}$, the data indicate that both $c_\pm(t)$ and $c_0(t)$ decay as $t^{-\alpha}$, where extrapolations of local slopes of neighboring points in Fig. 4(b) give $\alpha\cong 0.665$

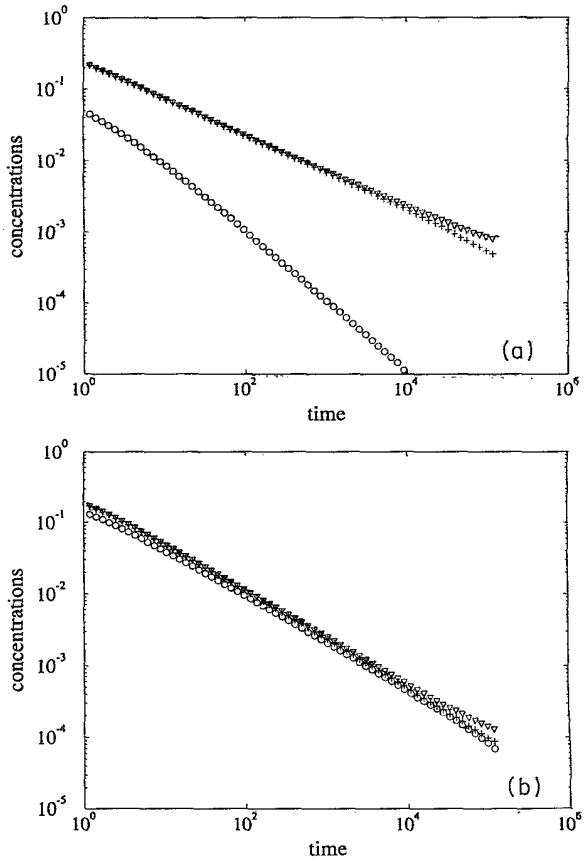

FIG. 4. Representative simulation results for the symmetric three-velocity in one dimension. Shown are double logarithmic plots of $c_+(t)$ (+), $c_-(t)$ (∇), and $c_0(t)$ (○) versus t for (a) $p_0=0.10$, $p_\pm=0.45$ and (b) at the tricritical point $p_0=0.25$, $p_\pm=0.375$. Each successive data point represents an increase in t by a factor of 1.2.

(Fig. 5). When the time difference between these points is the factor $1.2^{21}\approx 46$, a smooth sequence of local exponents is obtained. However, similar results are obtained for different choices of time delay factors. The trend in the local exponents suggests, in fact, that $\alpha=\frac{2}{3}$, a result that has now been obtained by an exact calculation [5]. Additionally, we estimate the relative amplitude $c_{\pm}(t)/c_0(t)\cong 1.17$. For $p_0>\frac{1}{4}$, $c_0(t)$ saturates to a finite limiting value that appears to be proportional to $(p_0-\frac{1}{4})^2$, while $c_{\pm}(t)$ decays faster than a power law in time. Based on these results, the phase diagram shown in Fig. 6 is inferred.

The location of the tricritical point, where all three species decay at the same rate, may be found by the following heuristic argument [8]. Since half the stationary particles react with + particles, the fraction of + particles available to react with − particles is simply $p_+-\frac{1}{2}p_0$. This is proportional to the number of $+-$ annihilation events per unit length P_{+-}. Similarly, the relative number P_{0-} of $0-$ annihilation events per unit length is equal to $\frac{1}{2}p_0$. Now we *assume* that $P_{+-}/P_{0-}=2$, based on the expectation that the relative number of annihilation events is proportional to the relative velocities of the collision partners. Combining the resulting relation $p_+-\frac{1}{2}p_0=p_0$ with the normalization condition $2p_++p_0=1$, we find the location of the tricritical point to be $p_0=\frac{1}{4}, p_+=p_-=\frac{3}{8}$.

It is straightforward to generalize this argument to the asymmetric velocity distribution $(+v,0,-1)$. Since the $+\leftrightarrow-$ symmetry is now broken, we must consider separately the ratios P_{+-}/P_{0-} and P_{-+}/P_{0+}. Following the same considerations as in the symmetric case, these reaction numbers are

$$\frac{P_{+-}}{P_{0-}}=\frac{p_+-vp_0/(1+v)}{p_0/(1+v)}=1+v\ ,$$
$$\frac{P_{-+}}{P_{0+}}=\frac{p_--p_0/(1+v)}{vp_0/(1+v)}=\frac{1+v}{v}\ . \tag{33}$$

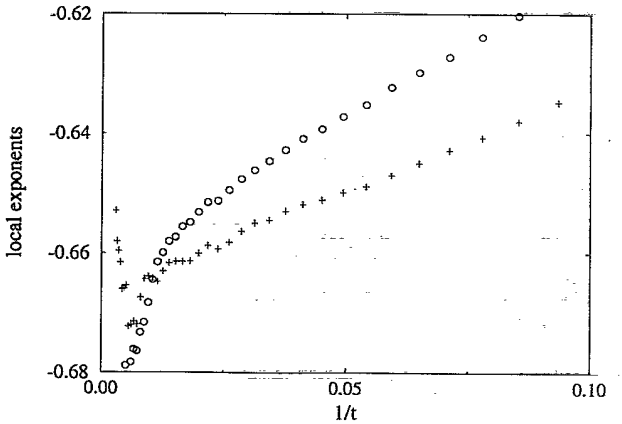

FIG. 5. Local exponents for $C(t)\equiv c_+(t)+c_-(t)$ (+) and $c_0(t)$ (○) versus $1/t$ at the tricritical point. These exponents are based on the slopes of points whose time difference is the factor $\tau=1.2^{21}\approx 46$ from the data of Fig. 4(b).

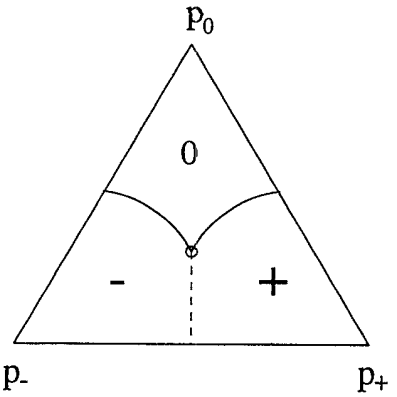

FIG. 6. Phase diagram of the symmetric three-velocity model in one dimension. Along the dashed line, $c_{\pm}(t)\sim t^{-1/2}$, while $c_0(t)\sim t^{-1}$. At the tricritical point (○), all species decay as $t^{-2/3}$. Along the solid lines, the nature of the decay is unknown, except very close to the extrema which correspond to the "fast impurity" problem (see the text).

Together with the normalization condition, we find, for the initial concentrations at the tricritical point,

$$p_0=\frac{1}{4},\quad p_+=\frac{1}{4}\left[1+\frac{v}{1+v}\right],\quad p_-=\frac{1}{4}\left[1+\frac{1}{1+v}\right]. \tag{34}$$

While Eq. (34) involves uncontrolled approximations, especially since symmetry considerations no longer apply, it is relatively accurate. For example, simulations with $v=2$ suggest that the tricritical point is located at $p_0\approx\frac{1}{4}$, and $p_+\approx 0.402$, compared to $p_+=\frac{5}{12}=0.41\overline{6}$ from Eq. (34). Generally when v varies from 0 to ∞, the tricritical point moves along the straight line parallel to the base of the composition triangle. At the extreme limits of $v=0$ and ∞ the three-velocity model degenerates to the two-velocity model for which we know that Eq. (34) is exact. The available numerical evidence also supports the apparent general equality $p_0=\frac{1}{4}$. Another interesting question in the general asymmetric case is whether the three coexistence curves really coalesce at one point or whether there is an open region where all concentrations decay at a similar rate. Numerics cannot answer such a question definitely, but the evidence appears to favor the hypothesis of one single tricritical point where all three coexistence lines merge.

Numerical results also suggest that near the tricritical point of the symmetric model $p_0=\frac{1}{4}$, $p_{\pm}=\frac{3}{8}$, the long-time kinetics depends on a single scaling variable $\xi\equiv t\Delta^3$, where $\Delta=p_0-\frac{1}{4}$ is assumed to be small. The scaling assumption for the concentrations gives

$$c_0(t,\Delta)\sim t^{-2/3}\mathcal{C}_0(t\Delta^3)\ ,$$
$$c_{\pm}(t,\Delta)\sim t^{-2/3}\mathcal{C}_{\pm}(t\Delta^3)\ , \tag{35}$$

with $\mathcal{C}_0(\xi)$ and $\mathcal{C}_{\pm}(\xi)$ finite at $\xi=0$ to reproduce the $t^{-2/3}$ decay at the tricritical point. This implies that $c_0(t,\Delta)\sim\Delta^2$, as is observed numerically. For $\Delta<0$ the scaling predictions agree with simulations if

$\mathcal{C}_0(\xi)\sim(-\xi)^{-1/3}$ and $\mathcal{C}_\pm(\xi)\sim(-\xi)^{1/6}$ as $\xi\to-\infty$. Thus scaling provides the Δ dependence of the asymptotic behavior for $\Delta<0$, namely, $c_0(t)\sim(t\Delta)^{-1}$ and $c_\pm(t)\sim(\Delta/t)^{1/2}$. Additionally, the crossover time from tricritical behavior to the final asymptotics scales as Δ^{-3}.

Since the concentration of stationary particles saturates to a finite value for $\Delta>0$, $\mathcal{C}_0(\xi)\sim\xi^{2/3}$ as $\xi\to\infty$. In this regime, $c_\pm(t)$ will eventually decay rapidly, presumably exponentially, leading to a similar decay of $\mathcal{C}_\pm(\xi)$ as $\xi\to\infty$. This has a remarkable consequence for the spatial distribution of immobile particles. Since the crossover time is of order Δ^{-3}, $c_\pm(t)$ should decay asymptotically as $\exp(-t\Delta^3)$. The residual concentration of the immobile particles, however, goes as Δ^2. The two facts appear contradictory, since the decay law for $c_\pm(t)$ implies that immobile-free intervals of length of order Δ^{-3} must be reasonably frequent. The resolution of this difficulty is presumably that immobile particles are distributed on a fractal set on length scales up to Δ^{-3}. A consistent value for the fractal dimension of this set is $\frac{1}{3}$, since this value indeed implies that there are Δ^{-1} particles in an interval of length Δ^{-3}. This observation has been verified numerically.

C. The impurity limit of the three-velocity model

When the concentration of one species is negligible while the other two species have equal concentrations, it is possible to determine the asymptotic survival probability of the "impurity." These results are worth emphasizing both for methodological interest and because of their unusual nature. First consider a stationary impurity in a background of $\pm$ particles. By the mutual annihilation of $\pm$ particles, their density decays as $c_\pm(t)\sim t^{-1/2}$. On the other hand, a stationary particle survives only if it is not annihilated by particles incident from either direction. Since each of these two events is independent, it follows that $c_0(t)\sim[c_\pm(t)]^2\sim t^{-1}$ in the limit $p_0\ll p_\pm$. This same argument continues to apply if the impurities are "slow," i.e., their velocity w satisfies $|w|<1$. The full survival probability is again a product of single-sided survival probabilities, each of which decays as $t^{-1/2}$.

More precisely, suppose that the impurity starts at the origin with velocity w and that there is a Poisson distribution of initial separations of the background particles. The impurity survival probability at time t, $S(t,w)$, equals the product of left- and right-sided survival probabilities $S_-(t,w)S_+(t,w)$. Since $S_-(t,w)\equiv S_+(t,-w)$, we only need to compute $S_+(t,w)$. This one-sided survival probability is given by

$$S_+(t,w)=\sum_{n=0}^{\infty} f_n P(x_{2n+1}>(1+w)t)\ . \tag{36}$$

This is simply the sum over all collisions partners of the probability that the collision time between the impurity and each of its potential collision partners is greater than t. For a Poisson distribution of interparticle separations with unit density, the probability that left-moving $(2n+1)$st particle is located at $x_{2n+1}>(1+w)t$ is

$$P(x_{2n+1}>(1+w)t)=\int_{(1+w)t}^{\infty}\frac{z^{2n}}{(2n)!}e^{-z}dz\ . \tag{37}$$

Combining Eqs. (32), (36), and (37) yields [9]

$$\begin{aligned}S_+(t,w)&=1-\int_0^{(1+w)t}e^{-z}I_1(z)\frac{dz}{z}\\&=e^{-(1-w)t}[I_0((1+w)t)+I_1((1+w)t)]\ .\end{aligned} \tag{38}$$

where I_1 is the modified Bessel function. Thus the complete survival probability is

$$\begin{aligned}S(t,w)&=e^{-2t}[I_0((1+w)t)+I_1((1+w)t)]\\&\quad\times[I_0((1-w)t)+I_1((1-w)t)]\\&\sim\frac{2}{\pi\sqrt{1-w^2}}t^{-1}\ ,\end{aligned} \tag{39}$$

in agreement with the rough argument given above.

Particularly intriguing behavior occurs in the complementary "fast" impurity limit with a vanishingly small initial concentration of + impurities in a background of equal concentrations of − and 0 particles. By a Galilean transformation, this system can be viewed as an impurity of velocity +3 in a +− background. More generally, we consider the decay of a fast impurity with speed $|w|>1$ in a +− background. An asymptotic argument suggests that this survival probability decays slower than an exponential but faster than a power law in time.

The basis of this argument is to consider a subset of configurations that gives the dominant contribution to the impurity survival probability, but is sufficiently simple to evaluate. For the impurity to survive to time t, the background $\pm$ particles must annihilate among themselves up to this time. On a space-time diagram, these self-annihilation events appear as a sequence of isosceles triangles that do not extend to the world line of the impurity. We posit that the dominant contribution to the survival probability stems from a sequence of systematically larger self-annihilation triangles that just miss the impurity world line (Fig. 7). From basic geometry, the base of the nth triangle x_n equals $x_0\beta^n$, with $\beta=(w+1)/(w-1)$. Here the separation between successive triangles is neglected, an approximation that is valid as the number (and size) of the triangles becomes large. Under this assumption of abutting triangles, the

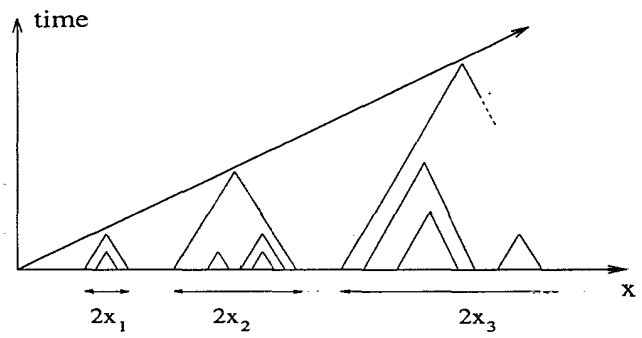

FIG. 7. World line of a fast impurity in a background of equal concentrations of background $\pm$ particles. Successive triangles of self-annihilating background particles are indicated.

number of such triangles that comprise the self-annihilation sequence up to time t is $N \simeq \ln(t/x_0)/\ln\beta$.

By construction, collision partners in the background define the sides of an individual self-annihilation triangle that encloses more local self-annihilation events. If these collision partners are separated by a distance x_n, the existence probability of the self-annihilation triangle is $(x_n/x_0)^{-3/2}$ as $n \to \infty$. The impurity survival probability $S(t)$ is therefore the product of occurrence probabilities for the sequence of self-annihilation triangles up to time t, leading to

$$S(t) \sim \prod_n^N (2x_0\beta^n)^{-3/2} \propto \beta^{-3N^2/4} \sim \exp[-\ln^2(t/x_0)/\tfrac{4}{3}\ln\beta] . \quad (40)$$

This result should be accurate when the number of self-annihilation triangles is large, a situation that occurs when $w \gtrsim 1$. In this limit, it is impractical to directly simulate the large systems needed to confirm the above prediction. We have therefore written a program that tracks *only* the impurity and the potential collision partners at any given stage of the reaction. Particles that are part of local self-annihilation events need not, and are not considered, leading to negligible CPU requirements. With this method we have simulated 10^7 realizations of an impurity with w as small as 1.0002. In this case, the mean impurity lifetime is approximately 340, but there are a few configurations with substantially longer lifetimes. For $w < 1.005$, a plot of the logarithm of the survival probability versus $z \equiv \ln^2(t)/\ln\beta$ exhibits good data collapse and relatively linear behavior over a substantial range (Fig. 8).

From $S(t)$ given in Eq. (40), the mean impurity lifetime $\langle t \rangle = \int^\infty S(t')dt'$ is readily computed to be proportional to $[(w+1)/(w-1)]^{2/3}$. While this is in excellent agreement with numerical results, the use of the asymptotic form for $S(t)$ even for t of order unity in the integral for $\langle t \rangle$ has yet to be justified. One additional amusing feature is that for $w \to 1+$, the probability that the impurity annihilates with a right-moving particle vanishes as $(w-1)^{1/2}$. When $w=1$, the impurity becomes one of the right-moving background particles, which can only annihilate with left-moving particles.

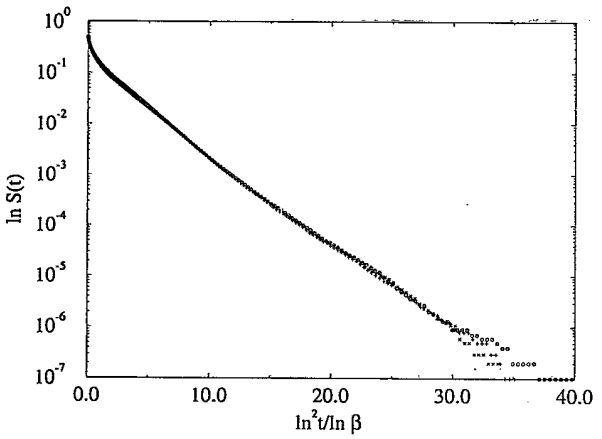

FIG. 8. Plot of the survival probability of a fast impurity. Shown is $\ln S(t)$ versus $\ln^2(t)/\ln\beta$ for $w-1=0.0005$, 0.001, and 0.002 (+, △, and ×, respectively).

D. The four-velocity model

We focus on the symmetric system with particles of velocities $\pm v_1$ and $\pm v_2$ and relative concentrations $p_1/2$ and $p_2/2$, respectively. According to the mean field description, the more rapid particles disappear more quickly for any $p_1, p_2 > 0$. However, we find three regimes of behavior in one dimension (Fig. 9). Depending on $\epsilon = v_1/v_2$, there is a critical value $p_1^*(\epsilon)$ such that for $p_1 < p_1^*(\epsilon)$, $c_1(t) \sim t^{-1}$, while $c_2(t) \sim t^{-1/2}$. The crossover to these asymptotic behaviors sets at progressively later times as p_1 approaches $p_1^*(\epsilon)$ from below. The converse behavior occurs for $p_1 > p_1^*(\epsilon)$. Roughly speaking, in these two cases the system reduces to the two-velocity model as the minority species disappears. However, when $p_1 = p_1^*(\epsilon)$ both species decay at the same rate. Based on extensive simulations, this decay appears to be a power law $t^{-\alpha}$, with $\alpha \cong 0.72 \pm 0.01$ (Fig. 9). This value is obtained by performing a least-squares fit to the data on a double logarithmic scale in the time range where linear behavior is most evident, typically for $10^2 \lesssim t \lesssim 10^4$. The error estimate is based on the variation of the exponent values for systems with p_1 within 0.01 of the critical value.

For detecting this power law behavior, direct molecular dynamics is once again inadequate. We therefore developed a more efficient algorithm, which can be viewed metaphorically as "pick up sticks." This approach is applicable for any initial velocity distribution with nondegenerate collision times. We first identify the collision times of all nearest-neighbor pairs and then sort them in ascending order by a standard $O(N \ln N)$ algorithm [10]. Next, these near-neighbor collision times are sequentially added to the list of true collision times if a consistency criterion, to be specified below, is satisfied. At each storage event, the particle pair $(n, n+1)$ associated with the underlying collision is removed from the system. Correspondingly, the collision times associated with $(n-1, n)$ and $(n+1, n+2)$ must be discarded, while the collision time associated with the new nearest-neighbor pair $(n-1, n+2)$ is computed. If any of these three collision times is smaller than the next near-neighbor collision time in the previously sorted list, it is necessary to re-sort the current list of collision times before continuing with the sequential storages of true collision times. Since the largest nearest-neighbor collision times will never be reached before re-sorting is necessary, the sorting is performed only on a small fraction of the smallest of these collision times at each stage. With this method we simulated 2.5×10^5 particles to 10^5 time steps in of the order of 70 CPU s on a DEC/AXP 3000/400 computer workstation. Our results are typically based on 50 realizations at each initial concentration.

The location of the critical point for the symmetric four-velocity model may also be estimated by the same

approach that was applied for the three-velocity model. Let P_{jj} be the number of annihilation events between $+$ and $-$ particles of type j, $j=1,2$, and let P_{ij}, $i\neq j$, be the number of annihilation events between, say, a $+$ particle of type i with both $+$ and $-$ particles of type j. There are two "mass" conservation laws $P_{22}+P_{21}\propto p_2$ and $P_{11}+P_{12}\propto p_1$, as well as the symmetry condition $P_{21}=P_{12}$. We further assume that $P_{22}/P_{21}=2$, indicative of the fact that the relative velocity between $+$ and $-v_2$ particles is equal to $2v_2$, while the average relative velocity between, say, a $+v_2$ particle and an arbitrary $\pm v_1$ particle is equal to v_2. Analogously, one also has $P_{11}/P_{12}=2v_1/v_2$. Combining these relations, the ratio of initial densities at the critical point is

$$\frac{p_2}{p_1}=\frac{3}{1+2v_1/v_2}\ . \tag{41}$$

Equation (41) reproduces the expected results in two extreme limits of $v_1=v_2$, where it gives $p_2=p_1$, while for

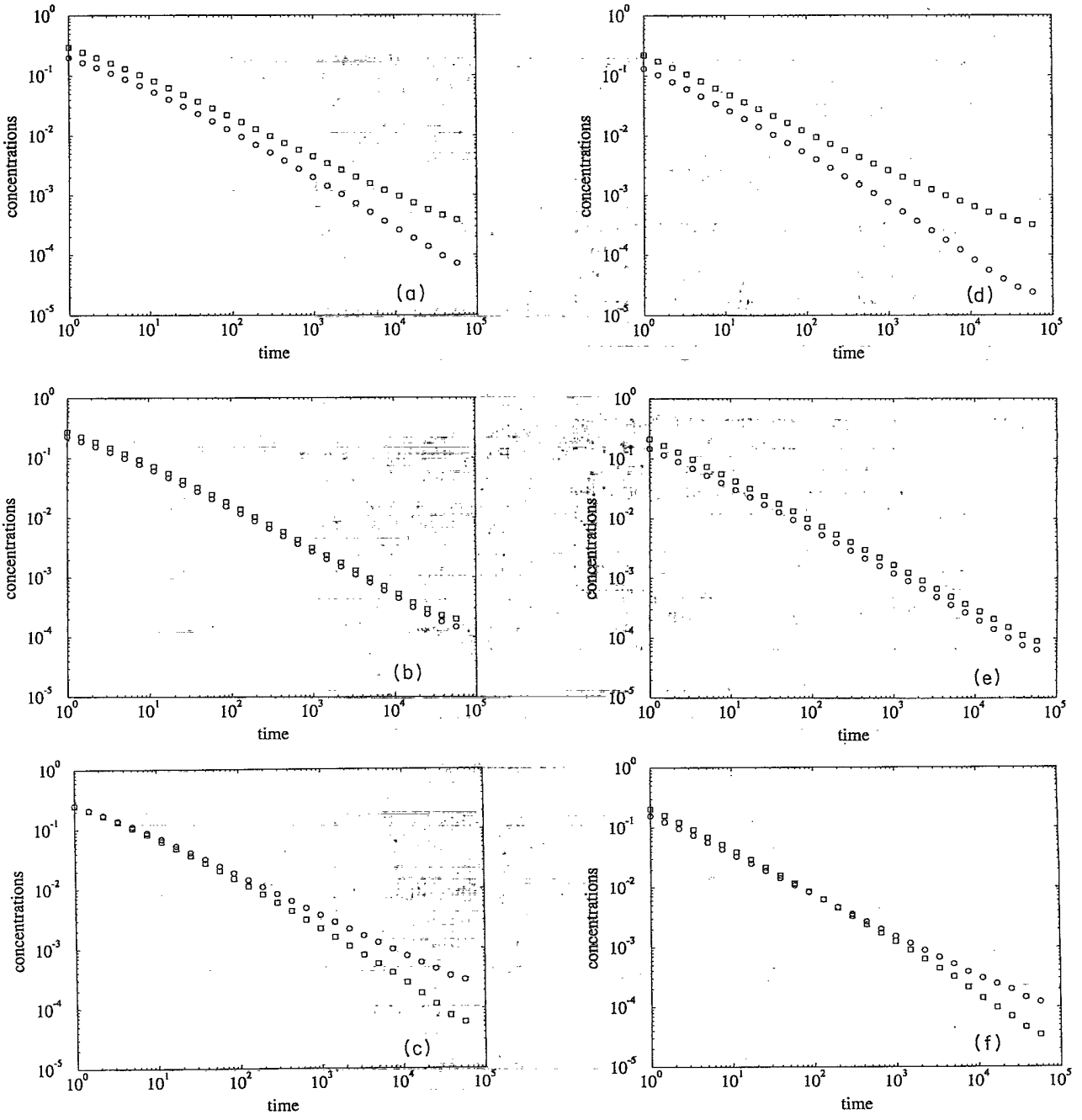

FIG. 9. Representative simulation results for the symmetric four-velocity in one dimension. Shown are a series of double logarithmic plots of $c_1(t)$ (□) and $c_2(t)$ (○) versus t for (a)–(c) $v_1=1$ and $v_2=1.1$ for $p_1=0.40$, 0.45, and 0.50, and (d)–(f) $v_1=1$ and $v_2=2$ for $p_1=0.35$, 0.38, and 0.40. Each successive data point represents an increase in t by a factor of 1.5.

$v_1=0$, the three-velocity tricritical point is reproduced. For two particular cases that were simulated extensively, Eq. (41) gives $p_2/p_1=1.5$ for $\epsilon=2$ and $p_2/p_1=1.065$ for $\epsilon=1.1$, while the corresponding estimates from simulations are 1.6 and 1.20. Thus, while Eq. (41) reproduces the correct qualitative trend for the location of the tricritical point, it is less accurate than the corresponding prediction of the three-velocity model.

V. SUMMARY

Ballistic annihilation when the particle velocities are drawn from discrete distributions is a problem that appears ripe for further exploration. There is a rich array of phenomena in which the underlying discreteness of the particle velocities is crucial. We have focused on simple and generic situations to elucidate these features. The mean field description of ballistic annihilation is deceptively simple, but leads to rather complex behavior. Particular attention was paid to distinguishing between the case of one-dimensional kinetics (which is the basis of conventional mean-field theory) and d-dimensional kinetics, in which averages over all particle directions in d dimensions is accounted for. Since the "number" of species is infinite, it is difficult to imagine that large-scale single-species heterogeneities could form. The absence of such spatial organization suggests that the mean field approximation is applicable when $d>1$.

In one dimension, the relative initial abundance of various species fundamentally determines which species predominates in the long-time limit. For the symmetric three-velocity model there is tricritical behavior in which all three species decay as $t^{-2/3}$ when $p_{\pm}=\frac{3}{8}$ and $p_0=\frac{1}{4}$. In the fast impurity limit, the survival probability of the impurity decays as $\exp(-\text{const}\times\ln^2 t)$. For the four-velocity model, mean field theory predicts that the faster species decays with a nonuniversal power law, while the slower species always decays as $1/t$. However, in one dimension, the relative initial concentrations again determine whether the more rapid or the slower species can dominate asymptotically. At the threshold between these two regimes, the densities of all species appears to decay at $t^{-\alpha}$, with $\alpha\cong 0.72$.

It is important to mention that Piasecki and Droz *et al.* have very recently developed a powerful analytic method to solve for the kinetics of one-dimensional of ballistic annihilation models exactly. In particular, they obtain the $t^{-2/3}$ decay for the density at the tricritical point of the symmetric three-velocity model that we inferred from simulations. Their method also appears to be applicable to general velocity distributions. However, even in the three-velocity model, the construction of explicit solutions from their formalism is a formidable task. Thus it still would be desirable to develop either continuum approaches or other analytical methods that would provide better intuitive insights into the intriguing qualitative features of ballistic annihilation.

ACKNOWLEDGMENTS

We thank E. Ben-Naim, M. Bramson, D. Dhar, L. Frachebourg, and I. Ispolatov for helpful discussions and correspondence. We also thank L. Frachebourg for informing us of related work prior to publication. We gratefully acknowledge ARO Grant No. DAAH04-93-G-0021, NSF Grants Nos. INT-8815438 and DMR-9219845, and the Donors of The Petroleum Research Fund, administered by the American Chemical Society, for partial support of this research.

[1] E. Ben-Naim, S. Redner, and F. Leyvraz, Phys. Rev. Lett. **70**, 1890 (1993).

[2] Y. Elskens and H. L. Frisch, Phys. Rev. A **31**, 3812 (1985); J. Krug and H. Spohn, *ibid.* **38**, 4271 (1988).

[3] A version of ballistic annihilation with a trimodal velocity distribution was introduced by W. S. Sheu, C. Van den Broeck, and K. Lindenberg, Phys. Rev. A **43**, 4401 (1991). However, the collision rules of this model were formulated to give behavior similar to that of the two-velocity model.

[4] Some aspects of the kinetics of ballistic annihilation with discrete velocity distributions were reported by S. Redner, in *Proceedings of the International Colloquium on Modern Quantum Field Theory II,* edited by G. Mandal (World Scientific, Singapore, 1994).

[5] Jarosław Piasecki, Phys. Rev. E **51**; M. Droz, P.-L. Rey, L. Frachebourg, and J. Piasecki, *ibid.* (to be published).

[6] P. L. Krapivsky, E. Ben-Naim, and S. Redner, Phys. Rev. E **50**, 2474 (1994).

[7] W. Feller, *An Introduction to Probability Theory and Its Applications* (Wiley, New York, 1968).

[8] E. Ben-Naim (private communication).

[9] *Handbook of Mathematical Functions,* edited by M. Abramowitz and I. A. Stegun (Dover, New York, 1964).

[10] W. H. Press, B. P. Flannery, S. A. Teukolsky, and W. T. Vetterling, *Numerical Recipes* (Cambridge University Press, Cambridge, England, 1986).